Organic & Biomolecular Chemistry

Cite this: *Org. Biomol. Chem.*, 2012, **10**, 3010

www.rsc.org/obc

PAPER

Fluorimetric detection of Mg^{2+} and DNA with 9-(alkoxyphenyl)benzo[*b*]-quinolizinium derivatives†

Maoqun Tian, Heiko Ihmels* and Shite Ye

Received 19th November 2011, Accepted 8th February 2012
DOI: 10.1039/c2ob06948b

A benzo[*b*]quinolizinium-benzo-15-crown-5 ether conjugate **2a** is presented that enables the fluorimetric detection of Mg^{2+} and DNA by a significant light-up effect, along with a change of the emission wavelength with different analytes (Mg^{2+}: 495 nm; DNA: 550 nm). The mechanism of the excited-state deactivation of **2a** was investigated by steady-state fluorescence spectroscopy in media of varied viscosity and compared with the photophysical properties of methoxyphenyl-substituted benzo[*b*]quinolizinium **2b** (*m*,*p*-diOMe), **2c** (*m*-OMe), and **2d** (*p*-OMe) as reference compounds. Compounds **2a–c**, which share the *m*-alkoxyphenyl substituent as the common feature, have low emission quantum yields ($\Phi_F < 10^{-2}$ in water) but exhibit a significant increase of their fluorescence intensity in viscous glycerol solutions. In contrast, the viscosity of the medium does not influence the emission properties of the parent phenyl-substituted benzo[*b*]quinolizinium **2e** and of the *p*-methoxyphenyl-substituted derivative **2d**. Based on these observations it is concluded that the excited-state deactivation in **2a–c** is mainly due to the rotation of the *m*-alkoxy group about the C_{ar}–O bond. The interaction of **2a–c** with DNA or Mg^{2+} ions was studied by spectrophotometric titrations and CD spectroscopy. Notably, the association of **2a** or **2b** with DNA or **2a** with Mg^{2+} ions induces a strong fluorescence enhancement (15- and 40-fold for DNA, 450-fold for Mg^{2+}), which is rationalized by the suppression of the torsional-relaxation of the alkoxy-substituent in the excited state. Additionally, the cation-induced light-up effect of **2a** is selective towards Mg^{2+} ions as compared with other cations such as NH_4^+, Li^+, Na^+, K^+ and Ba^{2+}.

Introduction

The detection of analytes with fluorescent probes is among the most useful and versatile techniques in different areas of chemistry,[1] because it offers the advantages of fluorescence spectroscopy combined with the high potential of chemical synthesis to provide almost any fluorophore with the required substitution pattern. Hence, numerous chemosensors have been developed for the fluorimetric detection of target analytes.[1] In a consequent development of this strategy, several bi- or multifunctional fluorescent probes have been designed that enable the detection of different analytes, ideally with analyte-specific emission properties.[2] Nevertheless, it is interesting to note that most of the latter probes focus on analytes from the same class of compounds, whereas probes that allow the optical detection of *different* types of analytes are rather rare.[3]

We have recently shown that the combination of the benzo[*b*]-quinolizinium fluorophore with appropriate receptor units enables the optical detection of metal cations, such as Hg^{2+}, Cu^{2+}, or Mg^{2+}, in most cases even in aqueous solution due to the high water solubility of the quinolizinium unit.[4] Furthermore, it has been demonstrated that the DNA-binding properties of the benzo[*b*]quinolizinium ligand may be employed in combination with a crown-ether receptor unit to detect Hg^{2+} and DNA simultaneously.[5] Encouraged by these results we aimed at the variation of this concept, *i.e.* by changing the receptor unit and its integration in the fluorophoric system in compound **2a**. We proposed that this compound may also be used as dual-pathway probe, that is, it likely exhibits, such as shown for **1**,[4c] low fluorescence quantum yield and may light up either upon association with DNA or by complexation of a fitting metal cation. Moreover, only the cation complexation should result in a significant change of the donor–acceptor interaction, such that the shift of the emission maximum is assumed to be different in the presence of cations or DNA, hence providing an additional tool for fluorimetric differentiation. Herein we present the synthesis and detailed investigation of the properties of **2a**, along with the

University of Siegen, Organic Chemistry II, Adolf-Reichwein-Str. 2, D-57068, Siegen, Germany. E-mail: ihmels@chemie.uni-siegen.de; Tel: +49 (0) 271 740 3440

†Electronic supplementary information (ESI) available: Fig. 3B, 6A, and 6B from main manuscript with enlarged insets; fluorimetric titration of Mg^{2+} to **2a**; Scatchard plots from photometric titrations of DNA to **2a**, **2b**, and **2c**; ^1H and ^{13}C NMR spectra of all new compounds. See DOI: 10.1039/c2ob06948b

comparative studies of reference compounds **2b–e** which revealed surprising results and a design principle for fluorescent light-up probes.

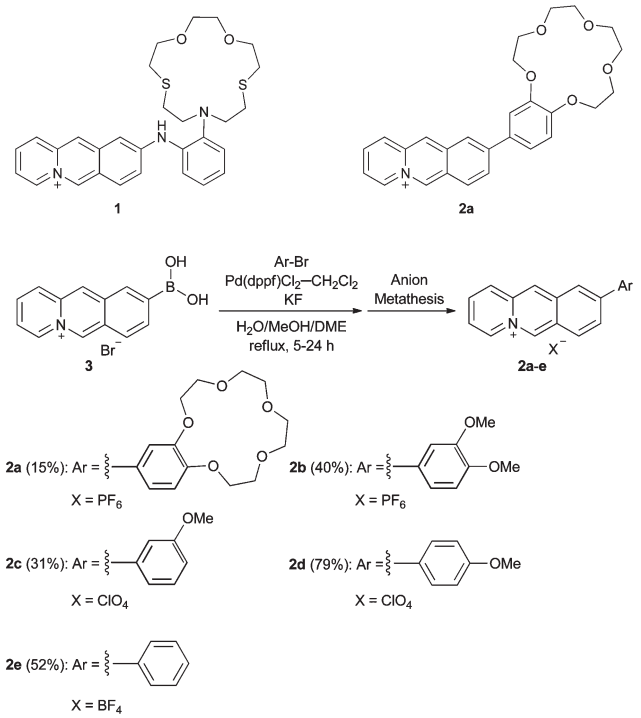

Scheme 1 Synthesis of benzo[*b*]quinolizinium derivatives **2a–e**.

Results

Synthesis

Benzo[*b*]quinolizinium derivatives **2a–e** were synthesized by Suzuki–Miyaura coupling reactions between 9-benzo[*b*]quinolizinium boronic acid (**3**) and bromoarenes (Scheme 1).[6] After counter-anion metathesis, the products were isolated in 15–79% yield as hexafluorophosphate, perchlorate or tetrafluoroborate salts. The structures of the new compounds **2a–c** were confirmed by ^{1}H- and ^{13}C-NMR spectroscopic analysis, mass-spectrometric and elemental analysis data. The known compounds **2d** and **2e** were identified by comparison of the NMR spectroscopic data with the literature data.[6]

Photophysical properties

A. Absorption and emission properties. The data of the absorption and emission properties of 9-arylbenzo[*b*]quinolizinium derivatives **2a–c** are presented in Fig. 1 and Table 1. All investigated compounds show weak solvatochromic properties, *i.e.*, depending on the solvent the maxima of the long-wavelength absorption are located between 409 nm and 430 nm. The dialkoxy-substituted derivatives **2a** and **2b** show broad, structureless and red-shifted absorption bands. The absorption bands of the *meta*-methoxy-substituted derivative **2c** are slightly more structured and closely resemble the ones of unsubstituted derivative **2e**.[6] Compounds **2a** and **2b** show very low fluorescence quantum yields (Φ_F < 0.01), whereas a slightly higher quantum yield (Φ_F = 0.01–0.04) of **2c** was observed in highly polar solvents, such as water, acetonitrile, methanol or DMF. Notably, the quantum yields of **2a** and **2b** increase significantly (Φ_F = 0.06–0.18) in chlorinated solvents such as dichloromethane or chloroform. The *meta*-methoxy substituted derivative **2c** exhibits a significantly blue-shifted emission spectra ($\Delta\lambda$ = 50–90 nm) as compared with the dialkoxy-substituted derivatives **2a** and **2b**.

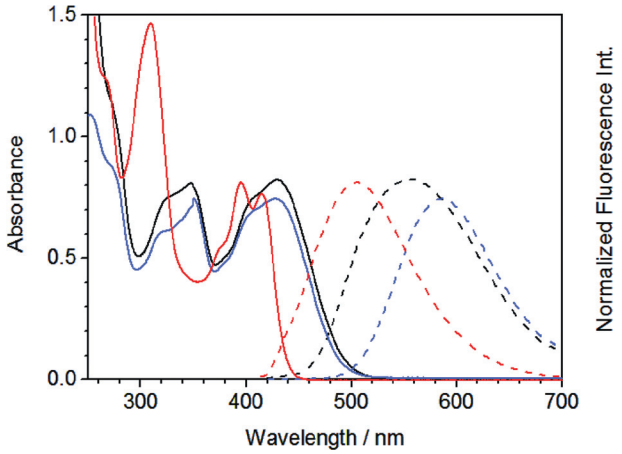

Fig. 1 Absorption and emission spectra of compounds **2a** (black), **2b** (blue) and **2c** (red) in CH_2Cl_2. Continuous lines: absorption spectra, c = 50 μM; dashed lines: normalized fluorescence spectra, c = 10 μM, λ_{ex} = 407 nm.

Table 1 Absorption and emission properties of compounds **2a–2c**

Compound	Solvent	λ_{abs}[a]/nm (log ε[b])	λ_F[c]/nm	Φ_F[d]/10^{-2}
2a	H_2O	412 (4.19)	—[e]	0.63
	MeCN	418 (4.15)	—[e]	1.0
	MeOH	418 (4.31)	—[e]	0.50
	DMF	420 (4.08)	—[e]	0.40
	CH_2Cl_2	430 (4.22)	559	7.9
	$CHCl_3$	424 (4.17)	544	5.8
	Glycerol	413 (4.20)	564	13
2b	H_2O	410 (4.13)	—[e]	0.14
	MeCN	417 (4.17)	—[e]	0.51
	MeOH	415 (4.19)	—[e]	0.50
	DMF	421 (4.03)	—[e]	0.52
	CH_2Cl_2	427 (4.17)	585	7.9
	$CHCl_3$	426 (4.17)	557	7.1
	Glycerol	411 (4.13)	560	7.7
2c	H_2O	409 (4.13)	453	0.66
	MeCN	415 (4.01)	459	3.6
	MeOH	411 (4.13)	460	2.1
	DMF	414 (3.85)	461	1.2
	CH_2Cl_2	415 (4.19)	506	16
	$CHCl_3$	415 (4.01)	466	18
	Glycerol	410 (4.13)	459	16

[a] Long-wavelength absorption maximum, c = 50 μM. [b] Extinction coefficient, in cm^{-1} M^{-1}. [c] Fluorescence emission maximum, c = 10 μM, λ_{ex} = 407 nm. [d] Fluorescence quantum yield relative to Coumarin 153 (ref. 7). [e] Too low to be determined.

B. Viscosity-dependent emission properties. The dependence of the fluorescence properties of **2a–c** on the viscosity of the medium was studied in glycerol–water mixtures with different

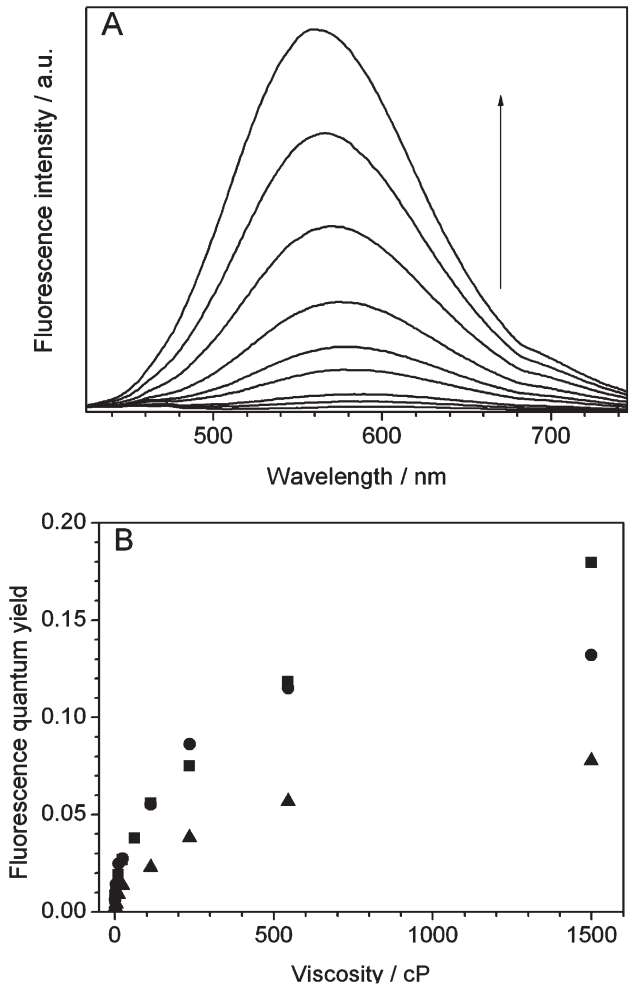

Fig. 2 A: Fluorescence spectra of compound **2a** in water–glycerol mixtures with different viscosity. The arrow indicates the development of the emission intensity with increasing the glycerol–water ratio (0–100%). B: Plot of fluorescence quantum yields of compounds **2a** (●), **2b** (▲) and **2c** (■) *versus* viscosity of the solution.

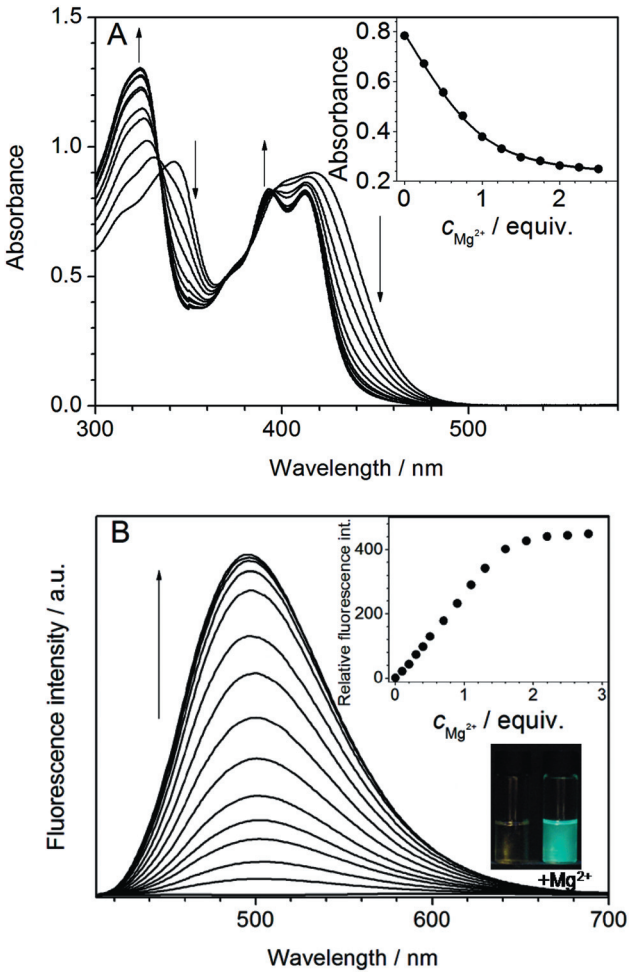

Fig. 3 Spectrophotometric (A) and spectrofluorimetric titration (B) of Mg^{2+} to compound **2a** (A: c = 50 μM; B: c = 10 μM, λ_{ex} = 395 nm) in MeCN. The arrows indicate the changes of absorption and emission upon addition of Mg^{2+}. Insets: Plot of the absorption at 430 nm (A) and emission intensity at 495 nm (B) *versus* Mg^{2+} concentration; numerical fits calculated for $K = 1.4 \times 10^5$ M^{-1} from photometric titration.

contents of the two components. These mixtures cover a broad range of viscosities; from η = 1.005 cP in water to 1499 cP in glycerol at 20 °C. In general, the fluorescence of compounds **2a–c** increases significantly, *i.e.* by a factor of 20 (**2a**), 55 (**2b**) and 24 (**2c**), with increasing glycerol content of the solution (Fig. 2, Table 1). In contrast, the unsubstituted derivative **2e** and the *p*-methoxy-substituted derivative **2d** displayed only insignificant variations of the emission properties upon changing the viscosity of the medium.

Interaction of the crown ether–quinolizinium conjugate 2a with Mg^{2+}

The interaction of the crown ether derivative **2a** with Mg^{2+} was investigated by photometric and fluorimetric titrations with $Mg(ClO_4)_2$ in MeCN (Fig. 3). The addition of Mg^{2+} to **2a** induced a significant blue shift of the broad structureless absorption band and the development of a well-structured band, which resembles the one of the 9-phenylbenzo[*b*]quinolizinium (**2e**). Simultaneously, several isosbestic points (335 nm, 382 nm, 395 nm) were observed, which slightly faded during the titration. At the same time, the fluorescence intensity of **2a** increased upon addition of Mg^{2+} by a factor of 450 with an emission maximum at 495 nm. The binding isotherm from the spectrophotometric titration was fitted to a 1 : 1 stoichiometry and the resulting binding constant of **2a**-Mg^{2+} was determined to be $K = 1.4 \times 10^5$ M^{-1}. In aqueous solutions an association of Mg^{2+} ions with the crown ether unit in **2a** was not detected because of the competing hydration.[8] Additionally, in aqueous media the lone electron pairs of the oxygen atoms of the crown ether point towards the exterior of the cyclic structure, such that a conformational change of the crown ether to establish a guest coordination is energetically less favourable.[9]

The selectivity of Mg^{2+}-induced light-up effect in **2a** was investigated by the determination of the fluorescence properties of **2a** in the presence of potentially competing cations such as NH_4^+, Li^+, Na^+, K^+, Ca^{2+}, or Ba^{2+} (10 equiv., resp.). No significant fluorescence enhancement was observed in the presence of NH_4^+, Na^+, or K^+, whereas the addition of Li^+, Ba^{2+}, and Ca^{2+} led to an increase of the fluorescence intensity by a factor of 8, 10, and 40 (Fig. 4).

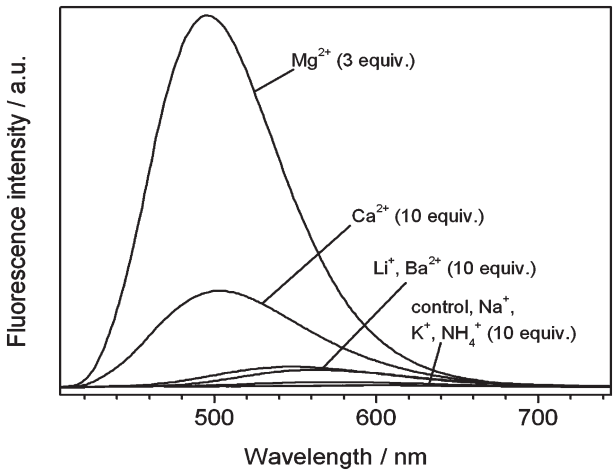

Fig. 4 The fluorescence spectra of **2a** (c = 10 μM) upon addition of Mg^{2+} (3 equiv.), Li^+, Na^+, K^+, Ca^{2+}, or Ba^{2+} (10 equiv., resp.).

Interaction of 2a, 2b and 2c with double stranded DNA

Derivatives **2a–c** show a similar behavior during photometric titrations with calf thymus DNA (ct DNA) in BPE buffer (Fig. 5). In each case, a decrease of the absorbance and a development of long-wavelength band were observed. At the same time, several isosbestic points (348 nm, 364 nm and 426 nm for **2a**, 318 nm, 351 nm and 417 nm for **2c**) were detected during the titration of DNA to **2a** and **2c**. In the case of **2b**, the isosbestic point at 439 nm faded when the concentration of DNA was larger than 30 μM (c_{ligand}/c_{DNA} < 1.6). In addition, the development of a long-wavelength absorption with a maximum at 422 nm was observed. For the evaluation of the DNA-binding constants and binding-site sizes, the data from spectrophotometric titrations were represented as Scatchard plot and fitted to the model of McGhee and von Hippel[10] to give the binding constant of **2a** and **2c** with DNA, $K = 8.2 \times 10^4$ M^{-1} (**2a**), 4.0×10^5 M^{-1} (**2c**) and the binding site size n = 1.5 (**2a**), 2.8 (**2c**). In the case of **2b**, only with c_{DNA} > 0.1 mM (c_{ligand}/c_{DNA} < 0.5) the corresponding Scatchard plot could be fitted satisfactorily with a binding constant $K = 1.6 \times 10^5$ M^{-1} and the binding site size n = 2.5. Attempts to fit the complete titration data to the model of McGhee and von Hippel or a two-side model[11] failed.

During the spectrofluorimetric titration of ct DNA to **2a** or **2b**, an enhancement of the fluorescence intensity at 550 nm or 575 nm by a factor of 15 or 40 was observed (Fig. 6A and 6B). In contrast, only a slight fluorescence enhancement (2-fold) was observed upon addition of DNA to **2c** (Fig. 6C).

The binding properties of **2a**, **2b** and **2c** with DNA were further investigated by circular dichroism (CD) spectroscopy (Fig. 7). Whereas aqueous solutions of the achiral compounds **2a**, **2b** and **2c** alone did not show any CD signals (Fig. 7A, line a), a positive induced CD (ICD) signal was observed in the long-wavelength absorption range of the ligand upon addition of DNA to **2a** (Fig. 7A, line b and c). In the case of **2b** a bisignate signal pattern was observed at very high ligand-to-DNA ratio of 5.0 (Fig. 7B, line b), whereas the CD spectrum of **2b** gave a strong positive ICD signal at lower ligand-to-DNA ratio of 0.1 (line c in Fig. 7B). In contrast, the ligand **2c** developed a negative ICD signal upon addition of ct DNA (Fig. 7C).

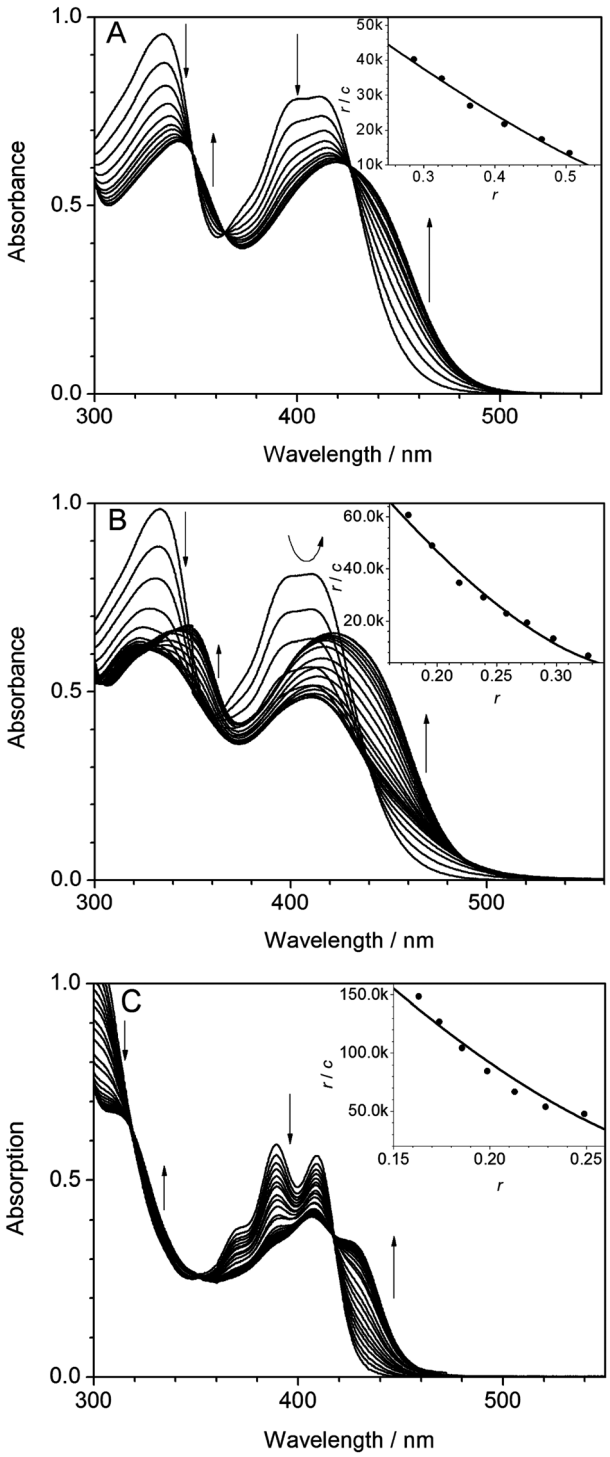

Fig. 5 Spectrophotometric titrations of **2a** (A), **2b** (B) and **2c** with ct DNA in BPE buffer (c = 50 μM). The arrows indicate the changes of the bands upon addition of ct DNA. Insets: Scatchard plots, r/c *versus* r; r = ligand-to-DNA ratio, fitted to the model of McGhee and von Hippel.

Discussion

Photophysical properties

The structureless absorption spectra of **2a** and **2b** and the expansion of the absorption band to >500 nm may be attributed to the

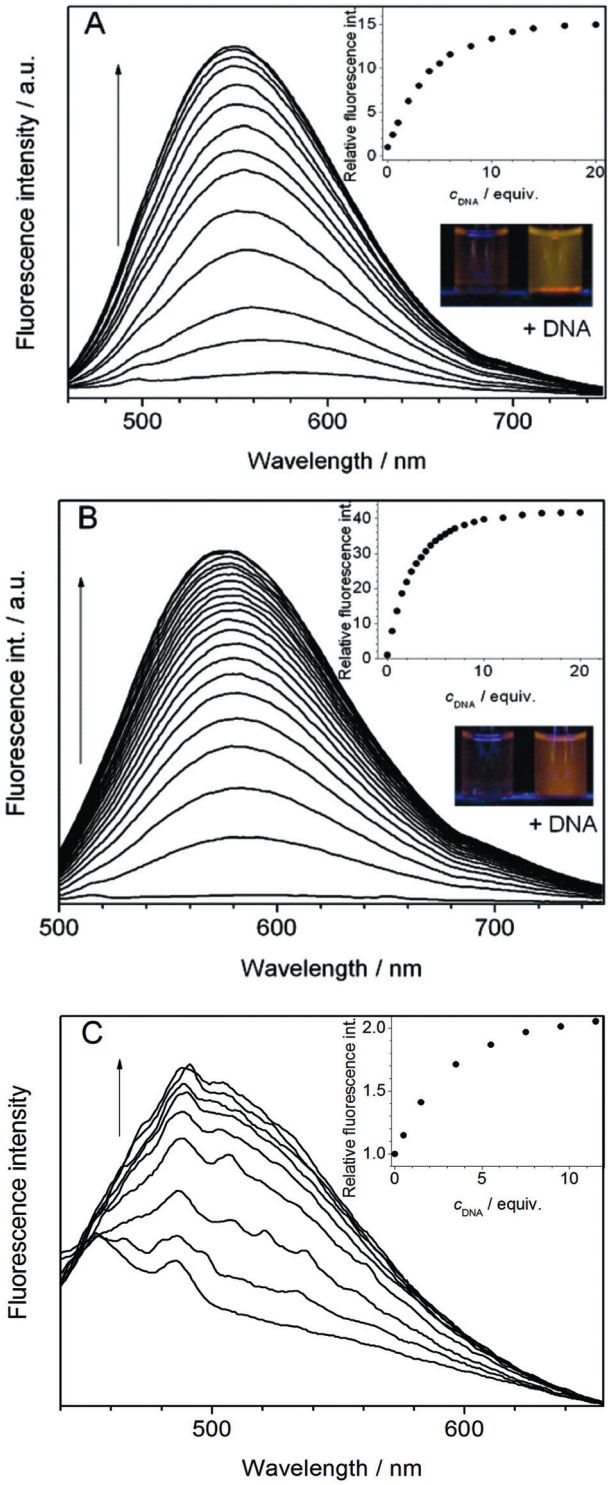

Fig. 6 Spectrofluorimetric titrations of **2a** (A, λ_{ex} = 425 nm), **2b** (B, λ_{ex} = 438 nm) and **2c** (C, λ_{ex} = 417 nm) with ct DNA in BPE buffer (c = 10 μM). The arrows indicate the changes of the bands upon addition of ct DNA. Insets: Plot of the relative emission intensity *versus* c_{DNA}.

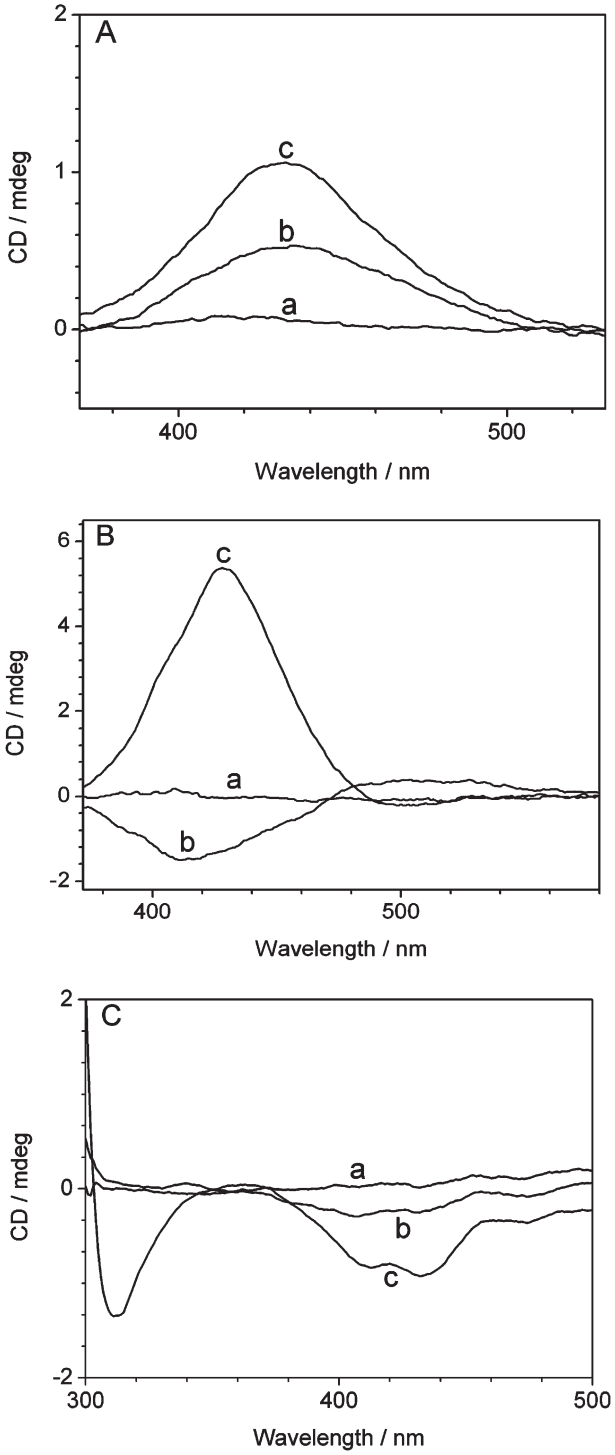

Fig. 7 A: CD spectra of **2a** (A), **2b** (B), and **2c** (C) in the absence (a) and presence of DNA; A: $c_{\mathbf{2a}}/c_{DNA}$ = 2.0 (b), $c_{\mathbf{2a}}/c_{DNA}$ = 0.2 (c). B: $c_{\mathbf{2b}}/c_{DNA}$ = 5.0 (b), $c_{\mathbf{2b}}/c_{DNA}$ = 0.1 (c). C: DNA $c_{\mathbf{2c}}/c_{DNA}$ = 1.0 (b), $c_{\mathbf{2c}}/c_{DNA}$ = 0.1 (c).

donor–acceptor interplay between the electron-rich methoxy-substituted phenyl substituent and the benzo[*b*]quinolizinium unit,[6] as commonly observed for donor–acceptor substituted chromophores.[12] In contrast, the absorption spectrum of **2c** has a blue-shifted zero onset (*ca*. 450 nm) and is more structured, thus resembling one of the unsubstituted derivative **2e**.[6] These photophysical properties of **2c** may be rationalized by the acceptor property of the *m*-methoxy group due to its −I effect, as indicated by the Hammett substituent constant (σ = 0.12). Other than the electron donating *p*-methoxy group (σ = −0.27)[13] a +M effect is not operative in *meta* position. The different extent of

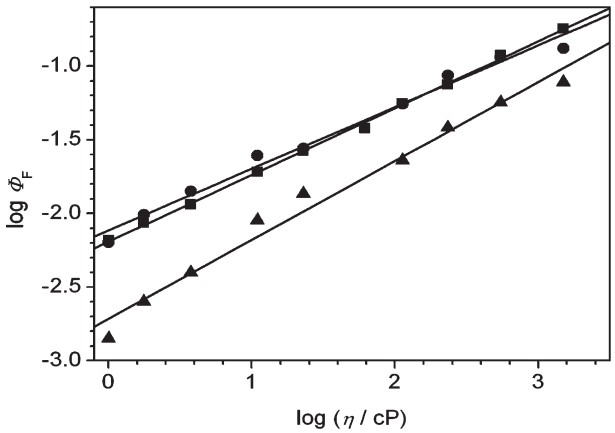

Fig. 8 Viscosity dependence of fluorescence quantum yields for **2a** (●), **2b** (▲) and **2c** (■). Slopes: k = 0.42 (r^2 = 0.99, **2a**), 0.54 (r^2 = 0.98, **2b**) and 0.45 (r^2 = 0.99, **2c**).

the donor–acceptor interaction in derivatives **2a–c** is also reflected in the emission spectra, *i.e.* the derivatives **2a** and **2b** with the stronger donor substituents exhibit a larger red-shift of the fluorescence maximum as compared with **2c**.

The benzo[*b*]quinolizinium derivatives **2a–c** have very low emission quantum yields with a remarkable increase in chlorinated solvents, such as dichloromethane and chloroform. Such an enhanced fluorescence quantum yield has been occasionally observed for cationic dyes and has been attributed to the high polarizability of these chlorinated solvents.[14] Notably, the fluorescence quantum yield of **2a–c** also increases with increasing viscosity of the medium, which indicates a radiationless deactivation of the excited state by conformational changes, as has been demonstrated already for 9-aminobenzo[*b*]quinolizinium derivatives, which undergo torsional relaxation about the N–C (aryl) bond.[14a] According to the Förster–Hoffmann equation such a relaxation process in the excited state is usually described by a linear relationship between Φ_F and η^k (eqn (1); with T = const., $\Phi_F \ll 1$).[15]

$$\Phi_F = C\eta^k \quad (1)$$

Indeed, in the case of **2a–c**, the double-logarithmic plot of the fluorescence quantum yields *versus* the viscosity of the medium is almost linear (Fig. 8). However, the slopes of the plots are significantly smaller (**2a**: k = 0.42; **2b**: k = 0.54; and **2c**: k = 0.45) than the ones derived theoretically for the rotation of the phenyl group (k = 2/3) and obtained experimentally *e.g.* for di- and triphenylmethane dyes.[16] This deviation from the theoretical value for the rotation of the phenyl indicates a different or an additional deactivation pathway for the excited state. In this regard it is to be noted that the viscosity of the medium does *not* influence the emission properties of compounds **2d** and **2e**. These observations indicate that the rotation of the phenyl group about the phenyl–aryl bond alone does not contribute significantly to the overall fluorescence quenching. At the same time, a rotation of the alkoxy substituents about the O–phenyl bond may be considered as deactivating process; but the marginal influence of the viscosity on the emission intensity of **2d** shows that at least for *para*-alkoxy substituents such an effect is not operative.

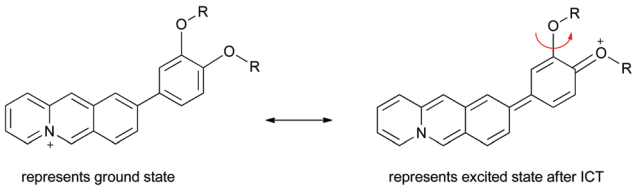

Scheme 2 Resonance structures of *p*-alkoxy-substituted 9-phenylbenzo[*b*]quinolizinium derivatives.

Presumably the rotation is hindered because a partial double bond character of the O–phenyl bond is developed due to excited-state charge transfer, as indicated by a quinoid resonance structure that represents the electron density distribution in the excited state (Scheme 2). As shown by the photophysical data, the *m*-alkoxy substituent does not act as electron donor, but rather as electron acceptor, mainly because it is not able to establish a linear conjugation with the positively charged quinolizinium nitrogen atom, so that the corresponding O–phenyl bond does not have any double bond character and can freely rotate. Based on these considerations, we conclude that the rotation of the *m*-alkoxy substituent constitutes a major contribution to the radiationless deactivation of the excited states of **2a–c**.

It should be noted, however, that the fluorescence of the 9-(4-*N*,*N*-dimethylamino)phenylaminobenzo[*b*]quinolizinium (**2f**) has been shown to be quenched by an intramolecular photoinduced electron transfer (PET) between the excited quinolizinium fluorophore and the aminophenyl donor unit.[6] Therefore it cannot be excluded that a similar PET takes place also in derivatives **2a–c**.

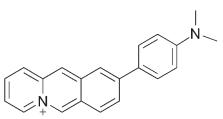

Interaction of benzocrown ether-substituted derivative 2a with Mg^{2+}

The formation of a well-structured and blue-shifted absorption band upon addition of Mg^{2+} to the solution of **2a** in MeCN indicates a significant suppression of the charge transfer from the electron rich phenyl ring to the benzo[*b*]quinolizinium chromophore (Fig. 3A). The isosbestic points that were observed during the photometric titration indicate that only one complex is formed between **2a** and Mg^{2+}. Furthermore, a 1 : 1 stoichiometry of the complex was supported by the good fit of the titration isotherm to the theoretical binding curve (r^2 = 0.999). The binding constant ($K = 1.4 \times 10^5$ M^{-1}) is comparable to the one of the known benzo-15-crown-5-Mg^{2+} complex ($K = 4.8 \times 10^4$ M^{-1}).[17]

Notably, the addition of Mg^{2+} to **2a** in MeCN induces a 450-fold enhancement of the fluorescence intensity (Fig. 3B), which is significantly blue-shifted (*ca.* 70 nm) compared with the fluorescence of **2a** in viscous medium such as glycerol. Thus, the fluorescence enhancement most likely originates from the suppression of the rotation of the *m*-alkoxy substituent by complexation of the benzocrown ether with Mg^{2+}. As a consequence, the fluorescence of **2a** is blue-shifted because of the disruption

of the donor–acceptor system by complexation with Mg^{2+} ions. The fluorescence response of **2a** towards Mg^{2+} ions is especially remarkable considering the tolerance of potentially competing alkali, alkaline earth cations or NH_4^+ (Fig. 4). This known selectivity for Mg^{2+} may be attributed to its relatively larger surface charge density,[18] which was shown in gas phase studies to be the dominant factor that determines the intrinsic metal ion affinity of crown ether receptors.[19] A similar effect has been found in biarylpyridine derivative.[20] In the latter case, however, the addition of acid efficiently quenches the fluorescence due to the formation of a TICT state, and the fluorescent enhancement caused by subsequent addition of metal cations is selective towards Mg^{2+} ions.

Interaction of derivatives 2a–c with ds DNA

The photometric titration of compound **2a** to DNA exhibits the characteristics of a DNA-binding process of cationic hetarenes, *i.e.* a hypochromic effect of the long-wavelength absorption band and the formation of red-shifted bands (Fig. 5A).[21] The isosbestic points are conserved during the titration, which indicates one almost exclusive binding mode. The binding constant of **2a** ($K = 8.2 \times 10^4\ M^{-1}$) is comparable to the ones of 9-donor substituted benzo[*b*]quinolizinium derivatives with DNA.[14a] At the same time, the positive ICD signal (Fig. 7A) is the result of a perpendicular orientation of the transition dipole moments of the ligand relative to the DNA binding site.[22] In analogy to the results obtained for a series of annelated quinolizinium derivatives[23] this ICD denotes a binding mode with the long molecular axes of the ligand perpendicular to the long axis of the intercalation binding site, since the transition dipole moment in **2a** is aligned almost parallel to the long molecule axis due to the donor–acceptor interplay within the chromophore. Overall the DNA-binding properties of **2a** resemble the ones observed for other cationic hetarenes that exhibit a high affinity towards nucleic acids.[24]

In the case of ligand **2b**, the DNA-binding process is more complicated (Fig. 5B). At lower DNA concentrations ($c_{DNA} \leq 30\ \mu M$), the change of the absorption bands is essentially identical to the one of the derivative **2a**. In particular, in this range of ligand-to-DNA ratios one isosbestic point at 439 nm reveals mainly one binding mode between the DNA and **2b**. Nevertheless, the loss of the isosbestic point and the development of the new long-wavelength absorption bands at higher DNA concentration ($c_{DNA} > 30\ \mu M$), *i.e.* lower ligand-to DNA ratio, indicate an additional binding mode between the ligand and DNA. The two different binding modes were also shown by the CD-spectroscopic experiments. Thus, at low ligand–DNA ratio ($c_{\mathbf{2b}}/c_{DNA} = 0.1$) a positive ICD signal was observed which is similar to the one of **2a**, so that a resembling intercalative binding mode may be deduced. This assumption is supported by the observation that the binding constants derived from the data of photometric titration at $c_{Ligand}/c_{DNA} < 0.5$ is comparable to the one of **2b**. At high ligand concentration ($c_{\mathbf{2b}}/c_{DNA} = 5.0$), however, the CD band develops into a bisignate ICD signal (Fig. 7B, line b) which is usually the result of exciton coupling from aggregates of the ligand that associate with the DNA backbone.[25] Overall, the data from spectrometric titrations of **2b** reveal that this compound intercalates into DNA at low ligand–DNA ratios *r*, whereas at higher *r* values this compound tends to form aggregates along the DNA backbone, as frequently observed for donor–acceptor substituted DNA binders.

During the photometric titration, the behaviour of **2c** is similar to that of **2a** (Fig. 5C), *i.e.* bathochromic and hypochromic effects, as well as formation of several isosbestic points. Moreover, compound **2c** exhibits a stronger interaction with DNA ($K = 4.0 \times 10^5\ M^{-1}$). The CD spectroscopic analysis, namely the development of a negative ICD signal, indicates the parallel alignment of the transition dipole moment of the ligand relative to the long axis of the binding pocket. The absorption and emission data of **2c** show that the *m*-phenyl substituent has only a marginal influence on the electronic situation of benzo[*b*]quinolizinium core, so that it may be concluded that the transition dipole moment of **2c** resembles the one of the parent benzo[*b*]-quinolizinium, *i.e.* slightly tilted from the short molecule axes.[26] Hence, the negative ICD indicates that **2c** is also bound to DNA by a perpendicular intercalation of the molecule into the binding site.

The fluorescence intensity of **2a** and **2b** increases significantly upon the interaction with DNA (Fig. 6A and 6B). The wavelengths of the emission maxima of **2a** and **2b** in the presence of DNA are close to the ones of **2a** and **2b** in glycerol ($\Delta\lambda_F \approx 15$ nm). Thus, it may be assumed that the intercalation of **2a** and **2b** with DNA restricts the conformational freedom of the ligands and thereby suppresses the main excited-state deactivation pathway. As the rotation of the 3-alkoxy substituent contributes significantly to the fluorescence quenching in the unbound ligand (see above), the enhancement of the fluorescence intensity of **2a** and **2b** is proposed to be mainly governed by the suppression of this torsional relaxation. The enhancement of the fluorescence is larger for **2a** (40-fold) than for **2b** (15-fold). This difference is consistent with the experimental results obtained for the viscosity-dependent fluorescence of these compounds (Table 1). However, only a slight fluorescence enhancement (2-fold) was observed upon addition of DNA to **2c**. Presumably, a photoinduced electron-transfer (PET) reaction between **2c** and nucleic base pairs quenches the fluorescence in the binding site. Presumably the PET is more pronounced in the case of **2c**, because the lack of donor–acceptor interplay as compared with **2a** and **2b** (see above) leads to a higher reduction potential in the excited state.[27]

Conclusions

Although fluorescent probes are known that selectively detect nucleic acids[28] or Mg^{2+} ions,[29] to the best of our knowledge, there are no reports on a probe molecule that is able to detect both analytes. Herein, we presented a benzo[*b*]quinoliziniumbenzo-15-crown-5 ether conjugate **2a** that enables the fluorimetric detection of Mg^{2+} and DNA by a significant light-up effect, along with an analyte-specific change of the emission wavelength. At the same time it is certainly a drawback of the presented system that due to the commonly known incompatibility of crown-ether receptors with aqueous media the detection of the separate analytes requires different solvents. Thus, it remains a challenge to modify the probe such that both analytes may be detected in the same medium. Nevertheless, with the present study it is shown in principle that the combination of the

benzo[*b*]quinolizinium fluorophore with appropriate receptor units may be used for the design of dual pathway probes. Moreover, the examination of the light-up mechanism by comparison with reference compounds **2b** and **2c** revealed a significant influence of the position of the methoxy functionality (*meta versus para*) on the emission properties of donor–acceptor systems. Overall, some principles are presented that may be employed generally for the development of efficient fluorescent probes.

Experimental

General instrumentations and materials

All commercially available chemicals were reagent grade and used without further purification. The melting point was determined with a Büchi 510K melting point apparatus and was not corrected. Mass spectra (ESI in the positive-ion mode, source voltage 6 kV) were recorded with a Finnigan LCQ Deca instrument; only *m*/*z* values in the range of 100–2000 units were analyzed. NMR spectra were measured on Varian NMR System 600 (^{1}H: 600 MHz, ^{13}C: 150 MHz) spectrometer at 20 °C; chemical shifts are given in ppm (δ) relative to TMS (δ = 0.00 ppm). Unambiguous proton NMR assignments were established by {1H, 1H}-COSY, HSQC and HMBC experiments. Elemental microanalysis was performed with a HEKAtech EuroEA combustion analyzer by Mr. H. Bodenstedt (Organische Chemie I, Universität Siegen). Purified water with resistivity ≥18 MΩ cm^{-1} was used for spectrometric measurements. 9-Benzo[*b*]-quinolizinium boronic acid (**3**), 9-(*p*-methoxyphenyl)benzo[*b*]-quinolizinium (**2d**) and 9-phenylbenzo[*b*]quinolizinium (**2e**) were prepared according to the literature procedure.[6]

Synthesis

General procedure for the synthesis of 9-arylbenzo[*b*]quinolizinium derivatives. Under inert-gas atmosphere, a solution of **3**[6] (303 mg, 1.00 mmol), the corresponding aryl bromide (1.50 mmol), Pd(dppf)Cl_2·CH_2Cl_2 (40.8 mg, 0.05 mmol) and KF (232 mg, 4.00 mmol) in DME–MeOH–H_2O (12 ml; 2 : 1 : 1) was stirred under reflux for 24 h (**2a**), 7 h (**2b**) or 12 h (**2c**). After cooling to r.t., MeOH (10 ml) was added to the reaction mixture and the formed precipitate was removed by filtration. A saturated aqueous solution of $NaPF_6$ or $NaClO_4$ (5 ml) was added to the filtrate until no more precipitation was observed. The yellow precipitate was collected, washed with water, EtOAc, and diethyl ether. The analytically pure product was separated by recrystallization of the precipitate from acetonitrile–ethyl acetate or by column chromatography (Al_2O_3, Activity I, eluent: MeCN) and subsequent recrystallization from acetonitrile–ethyl acetate.

9-(2,3,5,6,8,9,11,12-Octahydro-1,4,7,10,13-benzopentaoxacyclopentadecin-15-yl)-aminobenzo[*b*]quinolizinium hexafluorophosphate (2a). Yellow powder, yield 76 mg (15%); m. p. 113–114 °C (dec.); ^{1}H-NMR (600 MHz, [D_6]DMSO): δ = 3.64–3.67 (m, 8 H, CH_2), 3.81–3.85 (m, 4 H, CH_2), 4.15–4.25 (m, 4 H, CH_2), 7.15 (d, ^3J = 6 Hz, 1 H, H-Ph), 7.56–7.58 (m, 2 H, H-Ph), 7.89 (dd, ^3J = 6 Hz, ^3J = 6 Hz, 1 H, H-3), 8.02–8.03 (m, 1 H, H-2), 8.39–8.63 (m, 4 H, H-8, H-7, H-1, H-10), 9.07 (s, 1 H, H-11), 9.21 (d, ^3J = 6 Hz, 1 H, H-4), 10.33 (s, 1 H, H-6); ^{13}C-NMR (150 MHz, [D_6]DMSO): δ = 68.4 (CH_2), 68.6 (CH_2), 68.7 (CH_2), 68.8 (CH_2), 69.6 (CH_2), 69.7 (CH_2), 70.4 (CH_2), 70.5 (CH_2), 112.8 (CH_{ar}), 113.8 (CH_{ar}), 120.9 (CH_{ar}), 121.9 (C_q), 122.2 (CH_{ar}), 124.0 (C_q), 124.7 (CH_{ar}), 126.7 (CH_{ar}), 128.6 (C_q), 130.1 (CH_{ar}), 130.4 (CH_{ar}), 130.9 (CH_{ar}), 134.2 (CH_{ar}), 135.9 (CH_{ar}), 137.6 (C_q), 139.6 (CH_{ar}), 145.0 (C_q), 149.0 (C_q), 150.2 (C_q); MS (ESI$^+$): *m*/*z* (%) = 446 (100) [*M*]$^+$; elemental analysis calcd (%) for $C_{27}H_{28}F_6NO_5P$ (591.48): C, 54.83; H, 4.77; N, 2.37; found: C, 54.55; H, 4.32; N, 2.48.

9-(3,4-Dimethoxyphenyl)benzo[*b*]quinolizinium hexafluorophosphate (2b). Yellow powder, yield 175 mg (38%); m. p. 263–265 °C (dec.); ^{1}H-NMR (600 MHz, [D_6]DMSO): δ = 3.86 (s, 3 H, CH_3), 3.93 (s, 3 H, CH_3), 7.17–7.18 (m, 1 H, H-Ph), 7.56 (s, 1 H, H-Ph), 7.58–7.79 (m, 1 H, H-Ph), 7.89 (dd, ^3J = 7 Hz, ^3J = 7 Hz, 1 H, H-3), 8.02 (dd, ^3J = 7 Hz, ^3J = 7 Hz, 1 H, H-2), 8.41 (d, ^3J = 9 Hz, 1 H, H-8), 8.50 (d, ^3J = 9 Hz, 1 H, H-7), 8.54 (d, ^3J = 8 Hz, 1 H, H-1), 8.64 (s, 1 H, H-10), 9.10 (s, 1 H, H-11), 9.21 (d, ^3J = 7 Hz, 1 H, H-4), 10.34 (s, 1 H, H-6); ^{13}C-NMR (150 MHz, [D_6]DMSO): δ = 55.6 (CH_3), 55.8 (CH_3), 110.9 (CH_{ar}), 112.3 (CH_{ar}), 120.6 (CH_{ar}), 121.8 (CH_{ar}), 122.2 (CH_{ar}), 124.0 (CH_{ar}), 124.7 (C_q), 126.6 (CH_{ar}), 128.5 (CH_{ar}), 129.9 (C_q), 130.3 (CH_{ar}), 130.9 (CH_{ar}), 134.2 (CH_{ar}), 135.9 (C_q), 137.6 (C_q), 139.6 (CH_{ar}), 145.1 (C_q), 149.4 (C_q), 150.4 (C_q); MS (ESI$^+$): *m*/*z* (%) = 316 (100) [*M*]$^+$; elemental analysis calcd (%) for $C_{21}H_{18}F_6NO_2P$ (461.34): C, 54.67; H, 3.93; N, 3.04; found: C, 54.66; H, 3.69; N, 3.24.

9-(*m*-Methoxyphenyl)benzo[*b*]quinolizinium tetrafluoroborate (2c). Yellow powder, yield 116 mg (31%); m.p. 243–245 °C (dec.); ^{1}H-NMR (600 MHz, [D_6]DMSO): δ = 3.95 (s, 3 H, CH_3), 7.17–7.19 (m, 1 H, H-Ph), 7.57–7.60 (m, 3 H, H-Ph), 7.97–8.00 (m, 1 H, H-3), 8.10 (dd, ^3J = 8 Hz, ^3J = 8 Hz, 1 H, H-2), 8.42 (dd, ^3J = 9 Hz, ^4J = 2 Hz, 1 H, H-8), 8.59–8.64 (m, 2 H, H-7, H-1), 8.76 (s, 1 H, H-10), 9.22 (s, 1 H, H-11), 9.30 (d, ^3J = 7 Hz, 1 H, H-4), 10.45 (s, 1 H, H-6); ^{13}C-NMR (150 MHz, [D_6]DMSO): δ = 55.8 (CH_3), 113.5 (CH_{ar}), 115.6 (CH_{ar}), 120.4 (CH_{ar}), 122.6 (CH_{ar}), 124.2 (C_q), 125.0 (CH_{ar}), 125.5 (CH_{ar}), 127.2 (CH_{ar}), 129.2 (CH_{ar}), 131.0 (2 CH_{ar}), 131.5 (CH_{ar}), 134.7 (CH_{ar}), 136.1 (C_q), 138.1 (C_q), 139.6 (C_q), 140.3 (CH_{ar}), 145.5 (C_q), 160.4 (C_q); MS (ESI$^+$): *m*/*z* (%) = 286 (100) [*M*]$^+$; elemental analysis calcd (%) for $C_{20}H_{16}BF_4NO$ (373.15): C, 64.37; H, 4.32; N, 3.75; found: C, 63.79; H, 4.13; N, 3.94.

Spectrophotometric measurements

Absorption spectra were recorded on a Varian Cary 100 double-beam spectrophotometer; emission spectra were recorded on a Varian Cary Eclipse fluorescence spectrophotometer. All spectrophotometric measurements were performed in thermostated quartz sample cells at 20 °C. Solutions for analysis were prepared by dilution of stock solutions (1.0 × 10^{-3} M in water) immediately before the experiments. The solution concentrations were 50 μM for absorption and CD spectroscopy and 10 μM for fluorescence spectroscopy. Spectrophotometer slit widths were kept at 2 nm for absorption spectroscopy and 5/5 nm for emission spectroscopy. Titrations with Mg^{2+} or DNA: The solution

of the titrants $Mg(ClO_4)_2$ or ct DNA contained the appropriate concentration of the compound (to avoid dilution effects) and were added to a cuvette containing a solution of the compound in an appropriate buffer. The titration was monitored by absorption or emission spectroscopy. The titration was continued until no further changes in the spectrum were observed. All spectrophotometric measurements were performed at least three times to ensure reproducibility. Binding constants were determined by fitting the experimental binding isotherms to theoretical models according established procedures.[21a,30] to Circular dichroism (CD) spectra were recorded on a Chirascan (Applied Photophysics Limited, UK) apparatus.

Acknowledgements

Generous support by the *Deutsche Forschungsgemeinschaft* (FOR516) is gratefully acknowledged. We thank Ms. Laura Thomas for assistance with the determination of CD spectra.

Notes and references

1 (*a*) J. F. Zhang, Y. Zhou, J. Yoon and J. S. Kim, *Chem. Soc. Rev.*, 2011, **40**, 3416; (*b*) J. Wu, W. Liu, J. Ge, H. Zhang and P. Wang, *Chem. Soc. Rev.*, 2011, **40**, 3483; (*c*) M. E. Moragues, R. Martinez-Manez and F. Sancenon, *Chem. Soc. Rev.*, 2011, **40**, 2593; (*d*) R. M. Duke, E. B. Veale, F. M. Pfeffer, P. E. Kruger and T. Gunnlaugsson, *Chem. Soc. Rev.*, 2010, **39**, 3936; (*e*) M. Y. Berezin and S. Achilefu, *Chem. Rev.*, 2010, **110**, 2641; (*f*) J. Han and K. Burgess, *Chem. Rev.*, 2010, **110**, 2709; (*g*) H. Kobayashi, M. Ogawa, R. Alford, P. L. Choyke and Y. Urano, *Chem. Rev.*, 2010, **110**, 2620; (*h*) X. Qian, Y. Xiao, Y. Xu, X. Guo, J. Qiana and W. Zhua, *Chem. Commun.*, 2010, **46**, 6418; (*i*) R. W. Sinkeldam, N. J. Greco and Y. Tor, *Chem. Rev.*, 2010, **110**, 2579; (*j*) A. P. Demchenko, *Introduction to Fluorescence Sensing*, Springer, Berlin, 2009; (*k*) C. McDonagh, C. S. Burke and B. D. MacCraith, *Chem. Rev.*, 2008, **108**, 400; (*l*) A. P. de Silva, T. P. Vance, M. E. S. West and Glenn D. Wright, *Org. Biomol. Chem.*, 2008, **6**, 2468; (*m*) S. R. Adams, M. H. Ellisman and R. Y. Tsien, *Science*, 2006, **312**, 217; (*n*) L. Zhu and E. V. Anslyn, *Angew. Chem., Int. Ed.*, 2006, **45**, 1190; (*o*) L. Basabe-Desmonts, D. N. Reinhoudt and M. Crego-Calama, *Chem. Soc. Rev.*, 2007, **36**, 993.

2 (*a*) L. Zhu, L. Zhang and A. H. Younes, *Supramol. Chem.*, 2009, **21**, 268; (*b*) H.-H. Liu and Y. Chen, *Eur. J. Org. Chem.*, 2009, 5261; (*c*) M. Schmittel and H.-W. Lin, *Angew. Chem.*, 2007, **119**, 911; M. Schmittel and H.-W. Lin, *Angew. Chem., Int. Ed.*, 2007, **46**, 893 (*d*) Y. Q. Li, J. L. Bricks, U. Resch-Genger, M. Spieles and W. Rettig, *J. Phys. Chem. A*, 2006, **110**, 10972.

3 X. He and V. W.-W. Yam, *Org. Lett.*, 2011, **13**, 2172.

4 (*a*) M. Tian and H. Ihmels, *Chem. Commun.*, 2009, 3175; (*b*) M. Tian, H. Ihmels and E. Brötz, *Dalton Trans.*, 2010, **39**, 8195; (*c*) M. Tian and H. Ihmels, *Eur. J. Org. Chem.*, 2011, 4145.

5 M. Tian, H. Ihmels and K. Benner, *Chem. Commun.*, 2010, **46**, 5719.

6 M. Tian and H. Ihmels, *Synthesis*, 2009, 4226.

7 G. Jones, W. R. Jackson, C. Y. Choi and W. R. Bergmark, *J. Phys. Chem.*, 1985, **89**, 294.

8 C. J. Pedersen and H. K. Frensdorff, *Angew. Chem., Int. Ed. Engl.*, 1972, **11**, 16.

9 A. Späth and B. König, *Beilstein J. Org.Chem.*, 2010, **6**, 1.

10 J. D. McGhee and P. H. Von Hippel, *J. Mol. Biol.*, 1974, **86**, 469.

11 K. Bonjean, M. C. De Pauw-Gillet, M. P. Defresne, P. Colson, C. Houssier, L. Dassonneville, C. Bailly, R. Greimers, C. Wright, J. Quetin-Leclercq, M. Tits and L. Angenot, *Biochemistry*, 1998, **37**, 5136.

12 (*a*) J. N. Murrell, *The Theory of the Electronic Spectra of Organic Molecules*, John Wiley and Sons, New York, 1963; (*b*) R. Gompper and H.-U. Wagner, *Angew. Chem., Int. Ed. Engl.*, 1988, **27**, 1437.

13 C. Hansch, C. Leo and R. W. Taft, *Chem. Rev.*, 1991, **91**, 165.

14 (*a*) A. Granzhan, H. Ihmels and G. Viola, *J. Am. Chem. Soc.*, 2007, **129**, 1254; (*b*) O. van den Berg, W. F. Jager and S. J. Picken, *J. Org. Chem.*, 2006, **71**, 2666; (*c*) W. F. Jager, T. S. Hammink, O. van den Berg and F. C. Grozema, *J. Org. Chem.*, 2010, **75**, 2169; (*d*) L. Wu and K. Burgess, *J. Org. Chem.*, 2008, **73**, 8711.

15 T. Förster and G. Hoffmann, *Z. Phys. Chem.*, 1971, **75**, 63.

16 (*a*) G. Oster and Y. Nishijima, *J. Am. Chem. Soc.*, 1956, **78**, 1581; (*b*) M. Vogel and W. Rettig, *Ber. Bunsen-Ges. Phys. Chem.*, 1985, **89**, 962; (*c*) P. Gautam and A. Harriman, *J. Chem. Soc., Faraday Trans.*, 1994, **90**, 697.

17 C. Erk and A. Gocmen, *Talanta*, 2000, **53**, 137.

18 J. P. Geue, N. J. Head, A. D. Ward and S. F. Lincoln, *Dalton Trans.*, 2003, 521.

19 M. B. More, D. Ray and P. B. Armentrout, *J. Am. Chem. Soc.*, 1999, **121**, 417.

20 Y. Liu, M. Han, H.-Y. Zhang, L.-X. Yang and W. Jiang, *Org. Lett.*, 2008, **10**, 2873.

21 (*a*) D. E. Graves, Drug–DNA interactions, in *Methods in Molecular Biology, Vol. 95: DNA Topoisomerase Protocols: Volume II: Enzymology and Drugs*, ed. N. Osheroff and M. A. Bjornsti, Humana Press, Totowa, NJ, 2001, pp. 161–169; (*b*) H. Ihmels and D. Otto, *Top. Curr. Chem.*, 2005, **258**, 161.

22 B. Nordén and T. Kurucsev, *J. Mol. Recognit.*, 1994, **7**, 141.

23 H. Ihmels, K. Faulhaber, D. Vedaldi, F. Dall'Acqua and G. Viola, *Photochem. Photobiol.*, 2005, **81**, 1107.

24 For most recent examples, see *e.g.*: (*a*) R. B. P. Elmes, M. Erby, S. M. Cloonan, S. J. Quinn, D. C. Williams and T. Gunnlaugsson, *Chem. Commun.*, 2011, **47**, 686; (*b*) A. Mazzoli, B. Carlotti, C. Bonaccorso, C. G. Fortuna, U. Mazzucato, G. Miolo and A. Spalletti, *Photochem. Photobiol. Sci.*, 2011, **10**, 1830; (*c*) Z. Miskolczy, M. Megyesi, L. Biczók and Helmut Görner, *Photochem. Photobiol. Sci.*, 2011, **10**, 592; (*d*) T. Phillips, I. Haq and J. A. Thomas, *Org. Biomol. Chem.*, 2011, **9**, 3462.

25 H. Ihmels, K. Faulhaber, C. Sturm, G. Bringmann, K. Messer, N. Gabellini, D. Vedaldi and G. Viola, *Photochem. Photobiol.*, 2001, **74**, 505.

26 H. Ihmels, K. Faulhaber, B. Engels and C. Lennartz, *Chem.–Eur. J.*, 2000, **6**, 2854.

27 C. Bohne, K. Faulhaber, B. Giese, A. Häfner, A. Hofmann, H. Ihmels, A.-K. Köhler, S. Perä, F. Schneider and M. A. L. Sheepwash, *J. Am. Chem. Soc.*, 2005, **127**, 76.

28 For recent exemplary examples, see: (*a*) B. A. D. Neto and A. A. M. Lapis, *Molecules*, 2009, **14**, 1725; (*b*) T. Mahmood, A. Paul and S. Ladame, *J. Org. Chem.*, 2010, **75**, 204; (*c*) M. R. Gill, H. Derrat, C. G. W. Smythe, G. Battaglia and J. A. Thomas, *ChemBioChem*, 2011, **12**, 877; (*d*) J. Huang, Y. Wu, Y. Chen, Z. Zhu, X. Yang, C. J. Yang, K. Wang and W. Tan, *Angew. Chem., Int. Ed.*, 2011, **50**, 401; (*e*) L. J. Kricka and P. Fortina, *Clin. Chem.*, 2009, **55**, 670; (*f*) O. Vázquez, M. I. Sánchez, J. Martínez-Costas, M. E. Vázquez and J. L. Mascareñas, *Org. Lett.*, 2010, **12**, 216; (*g*) E. B. Veale and T. Gunnlaugsson, *J. Org. Chem.*, 2010, **75**, 5513; and references cited therein.

29 For recent exemplary examples, see: (*a*) Y. Dong, J. Li, X. Jiang, F. Song, Y. Cheng and C. Zhu, *Org. Lett.*, 2011, **13**, 2252; (*b*) J. Brandel, M. Sairenji, K. Ichikawa and T. Nabeshima, *Chem. Commun.*, 2010, **46**, 3958; (*c*) M. Ishida, Y. Naruta and Fumito Tani, *Angew. Chem., Int. Ed.*, 2010, **122**, 95; (*d*) Y. Liu, M. Han, H.-Y. Zhang, L.-X. Yang and Wei Jiang, *Org. Lett.*, 2008, **10**, 2873; (*e*) H. M. Kim, P. R. Yang, M. S. Seo, J. S. Yi, J. H. Hong, S.-J. Jeon, Y.-G. Ko, K. J. Lee and B. R. Cho, *J. Org. Chem.*, 2007, **72**, 2088; (*f*) D. Ray and P. K. Bharadwaj, *Inorg. Chem.*, 2008, **47**, 2252; and references cited therein.

30 (*a*) B. Valeur, *Molecular Fluorescence: Principles and Applications*, Wiley-VCH, Weinheim, 2002; (*b*) J. Polster and H. Lachmann, *Spectrometric Titrations: Analysis of Chemical Equilibria*, VCH, Weinheim, 1989.

